Hindawi Publishing Corporation
ISRN Mechanical Engineering
Volume 2014, Article ID 764837, 10 pages
http://dx.doi.org/10.1155/2014/764837

Research Article

Elastic Analysis of Rotating Thick Truncated Conical Shells Subjected to Uniform Pressure Using Disk Form Multilayers

Mohammad Zamani Nejad,[1] Mehdi Jabbari,[1] and Mehdi Ghannad[2]

[1] *Mechanical Engineering Department, Yasouj University, P.O. Box 75914-353, Yasouj, Iran*
[2] *Mechanical Engineering Faculty, Shahrood University of Technology, Shahrood, Iran*

Correspondence should be addressed to Mohammad Zamani Nejad; m.zamani.n@gmail.com

Received 20 December 2013; Accepted 20 February 2014; Published 17 March 2014

Academic Editors: S. Shen and A. Tounsi

Using disk form multilayers, an elastic analysis is presented for determination of displacements and stresses of rotating thick truncated conical shells. The cone is divided into disk layers form with their thickness corresponding to the thickness of the cone. Due to the existence of shear stress in the truncated cone, the equations governing disk layers are obtained based on first shear deformation theory (FSDT). These equations are in the form of a set of general differential equations. Given that the truncated cone is divided into n disks, n sets of differential equations are obtained. The solution of this set of equations, applying the boundary conditions and continuity conditions between the layers, yields displacements and stresses. The results obtained have been compared with those obtained through the analytical solution and the numerical solution.

1. Introduction

Scientists have paid an enormous amount of attention to shells, resulting in numerous theories about their behavior of different kinds of shells. Truncated conical shells have widely been applied in many fields such as space fight, rocket, aviation, and submarine technology. The literature that addresses the stresses of thick conical shells is quite limited. Most of the existing literature deals with the stress or vibration analysis of thin conical shells and is based upon a thin shell or membrane shell theory. Using the first shear deformation theory, Mirsky and Hermann [1] derived the solution of thick cylindrical shells of homogenous and isotropic materials. Assuming the cone is to be long and the angle of the lateral side with a horizontal plane is great, Hausenbauer and Lee [2] without considering shear stresses obtained the radial, tangential, and axial wall stresses in a thick-walled cone under internal and/or external pressure. Raju et al. [3] introduced a conical element for analysis of conical shells. Using the shear deformation theory and Frobenius series, Takahashi et al. [4] obtained the solution of free vibration of conical shells. Sundarasivarao and Ganesan [5] analyzed a conical shell under pressure using the finite element method. Based on bending theory, Tavares [6] determined the stresses, strains, and displacements of a thin conical shell with constant thickness and axisymmetric load by the construction of a Green's function. Cui et al. [7] used a new transformation for solving the governing equations of thin conical shells. The obtained equation is an ordinary differential equation with complex coefficients. Wu and Chiu [8] investigated thermally induced dynamic instability of laminated composite conical shells subjected to static and periodic thermal loads by means of the multiple scales method of perturbation theory. Pinto Correia et al. [9] used the FEM for analysis of a composite conical shell where the shear deformation theory has been used for formulation. Jane and Wu [10] studied thermoelasticity problem in the curvilinear circular conical coordinate system. The hybrid Laplace transformation and finite difference were developed to obtain the solution of two-dimensional axisymmetric coupled thermoelastic equations. Wu et al. [11] presented the three-dimensional solution of laminated conical shells subjected to axisymmetric loadings using the method of perturbation. Eipakchi et al. [12] used the mathematical approach based on the perturbation theory,

for elastic analysis of a thick conical shell with varying thickness under nonuniform internal pressure. Based on first shear deformation theory and the virtual work principle, Ghannad et al. [13] obtained an elastic solution for thick truncated conical shells. Using the tensor analysis, Nejad et al. [14] obtained a complete and consistent 3D set of field equations to characterize the behavior of FGM thick shells of revolution with arbitrary curvature and variable thickness. Deformations and stresses inside multilayered thick-walled spheres are investigated by Borisov [15]. In the paper, each sphere is characterized by its elastic modules. Using third-order shear deformation theory, an analytical solution presented for stresses and displacements in a thick conical shell with varying thickness under nonuniform internal pressure [16]. The finite element method based on the Rayleigh-Ritz energy formulation is applied to obtain the elastic behavior of the functionally graded thick truncated cone [17]. Making use of FSDT and the virtual work principle, Ghannad and Zamani Nejad [18] generally derived the governing differential equations of the homogenous and isotropic axisymmetric thick-walled cylinders with same boundary conditions at the two ends. Shadmehri et al. [19] proposed a semianalytical approach to obtain the linear buckling response of conical composite shells under axial compression load. The principle of minimum total potential energy was used to obtain the governing equations and Ritz method was applied to solve them. Free vibration analysis of laminated conical shells is presented by Civalek [20]. He provided results for isotropic, orthotropic, and laminated cases for conical shells by using the numerical solution of governing differential equations of motion based on transverse shear deformation theory. Using disk form multilayers, Nejad et al. [21] derived a semianalytical solution for determination of displacements and stresses in a rotating cylindrical shell with variable thickness under uniform pressure.

In the present study, on has the following.

(1) Based on FSDT and elasticity theory, the governing equations of thick-walled disks are derived.

(2) Thick truncated cone is divided into disks with constant thickness and constant height.

(3) With considering continuity between layers and applying boundary conditions, the governing set of differential equations with constant coefficients is solved.

(4) The results obtained for stresses and displacements are compared with the solutions carried out through the FEM. Good agreement was found among the results.

2. Formulation of Problem

In the first-order shear deformation theory, the sections that are straight and perpendicular to the mid-plane remain straight but not necessarily perpendicular after deformation and loading. In this case, shear strain and shear stress are taken into consideration.

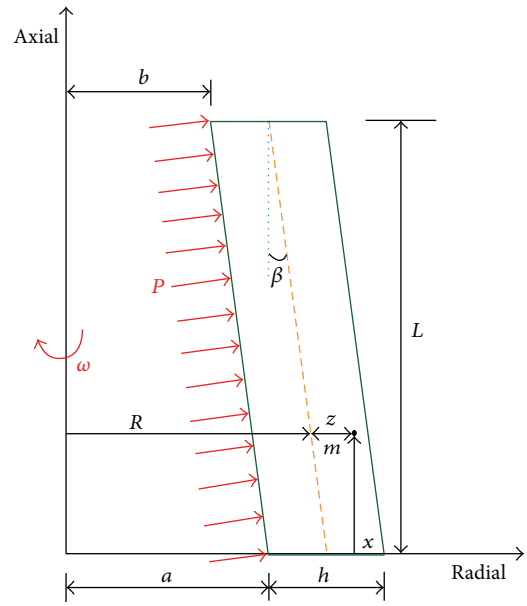

Figure 1: Geometry of thick-walled truncated cone.

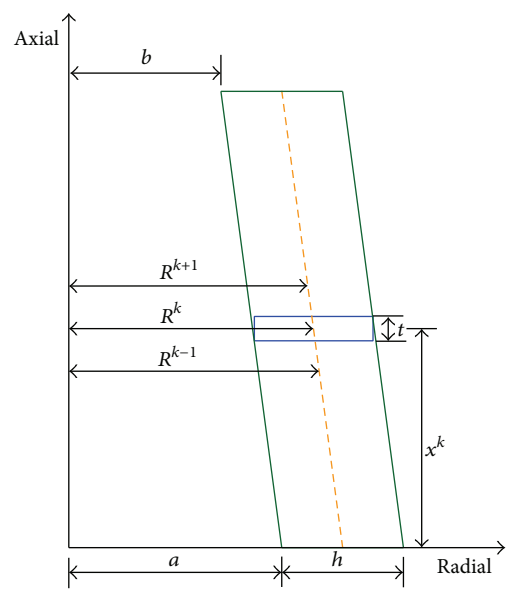

Figure 2: Dividing of truncated cone to disk form multilayer.

Geometry of a thick truncated cone with thickness h and the length L is shown in Figure 1.

The location of a typical point m, within the shell element, is as

$$m : (r, x) = (R + z, x),$$
$$0 \le x \le L, \qquad -\frac{h}{2} \le z \le \frac{h}{2}, \tag{1}$$

where z is the distance of typical point from the middle surface. In (1), R represents the distance of middle surface from the axial direction

$$R(x) = a + \frac{h}{2} - (\tan\beta)\, x, \tag{2}$$

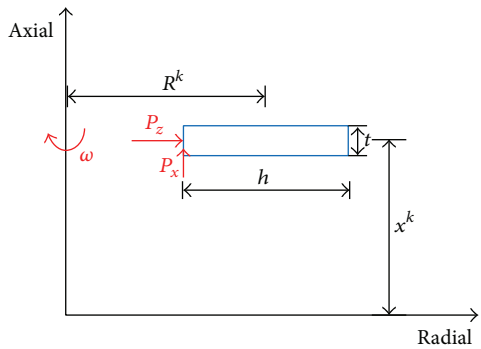

FIGURE 3: Geometry of an arbitrary disk layer.

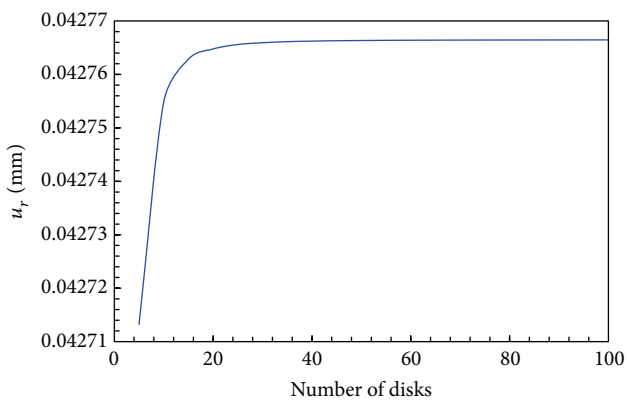

FIGURE 4: Effect of the number of disk layers on the radial displacement.

where β is half of tapering angle as

$$\beta = \tan^{-1}\left(\frac{a-b}{L}\right). \tag{3}$$

Applied pressure to internal surface includes two components as follows:

$$P_x = P\sin\beta, \qquad P_z = P\cos\beta, \tag{4}$$

where P_x and P_z are components of internal pressure P along axial and radial directions, respectively.

The general axisymmetric displacement field (U_x, U_z), in the first-order Mirsky-Hermann's theory [1], could be expressed on the basis of axial displacement and radial displacement as follows:

$$U_x(x,z) = u(x) + \phi(x)z, \qquad U_z(x,z) = w(x) + \psi(x)z, \tag{5}$$

where $u(x)$ and $w(x)$ are the displacement components of the middle surface. Also, $\phi(x)$ and $\psi(x)$ are the functions used to determine the displacement field.

The kinematic equations (strain-displacement relations) in the cylindrical coordinates system are

$$\begin{aligned}
\varepsilon_x &= \frac{\partial U_x}{\partial x} = \frac{du}{dx} + \frac{d\phi}{dx}z,\\
\varepsilon_\theta &= \frac{U_z}{r} = \left(\frac{w}{R+z}\right) + \left(\frac{\psi}{R+z}\right)z,\\
\varepsilon_z &= \frac{\partial U_z}{\partial z} = \psi,\\
\gamma_{xz} &= \frac{\partial U_x}{\partial z} + \frac{\partial U_z}{\partial x} = \left(\phi + \frac{dw}{dx}\right) + \frac{d\psi}{dx}z.
\end{aligned} \tag{6}$$

The stress-strain relations (constitutive equations) for homogeneous and isotropic materials are as follows:

$$\begin{Bmatrix} \sigma_x \\ \sigma_\theta \\ \sigma_z \\ \tau_{xz} \end{Bmatrix} = \lambda \begin{bmatrix} 1-\upsilon & \upsilon & \upsilon & 0 \\ \upsilon & 1-\upsilon & \upsilon & 0 \\ \upsilon & \upsilon & 1-\upsilon & 0 \\ 0 & 0 & 0 & \dfrac{1-2\upsilon}{2} \end{bmatrix} \begin{Bmatrix} \varepsilon_x \\ \varepsilon_\theta \\ \varepsilon_z \\ \gamma_{xz} \end{Bmatrix}, \tag{7}$$

where σ_i and ε_i, $i = x, \theta, z$, are the stresses and strains in the axial (x), circumferential (θ), and radial (z) directions. υ and E are Poisson's ratio and modulus of elasticity, respectively. In (6), λ is

$$\lambda = \frac{E}{(1+\upsilon)(1-2\upsilon)}. \tag{8}$$

The normal forces (N_x, N_θ, N_z), bending moments (M_x, M_θ, M_z), shear force (Q_x), and the torsional moment (M_{xz}) in terms of stress resultants are

$$\begin{aligned}
\begin{Bmatrix} N_x \\ N_\theta \\ N_z \end{Bmatrix} &= \int_{-h/2}^{h/2} \begin{Bmatrix} \sigma_x\left(1+\dfrac{z}{R}\right) \\ \sigma_\theta \\ \sigma_z\left(1+\dfrac{z}{R}\right) \end{Bmatrix} dz,\\
\begin{Bmatrix} M_x \\ M_\theta \\ M_z \end{Bmatrix} &= \int_{-h/2}^{h/2} \begin{Bmatrix} \sigma_x\left(1+\dfrac{z}{R}\right) \\ \sigma_\theta \\ \sigma_z\left(1+\dfrac{z}{R}\right) \end{Bmatrix} z\,dz,\\
Q_x &= K\int_{-h/2}^{h/2} \tau_{xz}\left(1+\frac{z}{R}\right)dz,\\
M_{xz} &= K\int_{-h/2}^{h/2} \tau_{xz}\left(1+\frac{z}{R}\right)z\,dz,
\end{aligned} \tag{9}$$

where K is the shear correction factor that is embedded in the shear stress term. In the static state, for conical shells $K = 5/6$ [22].

On the basis of the principle of virtual work, the variations of strain energy are equal to the variations of work of external forces as follows:

$$\delta U = \delta W, \tag{10}$$

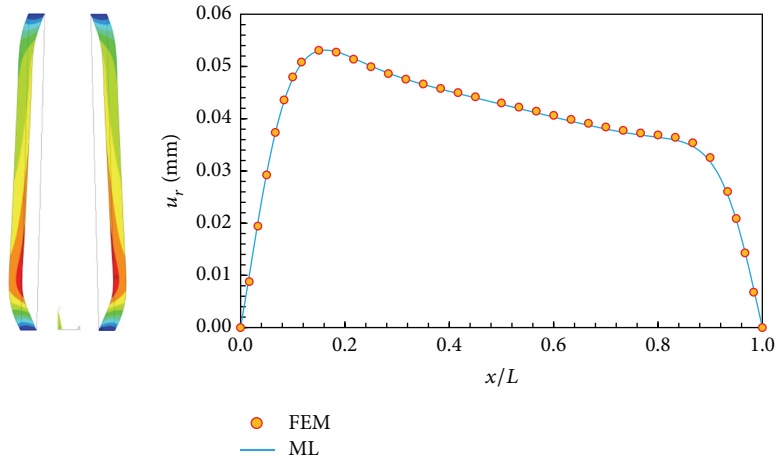

Figure 5: Radial displacement distribution in middle layer.

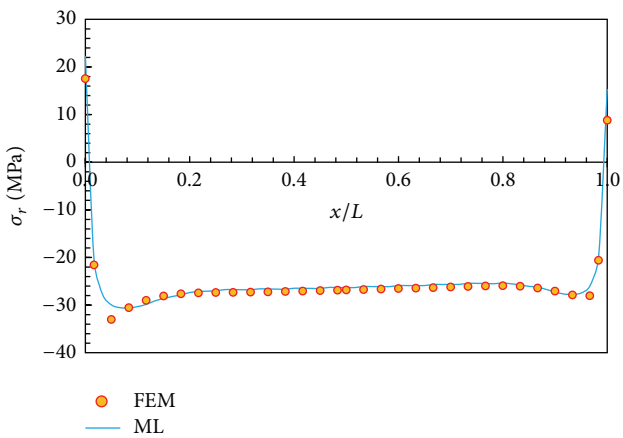

Figure 6: Radial stress distribution in middle layer.

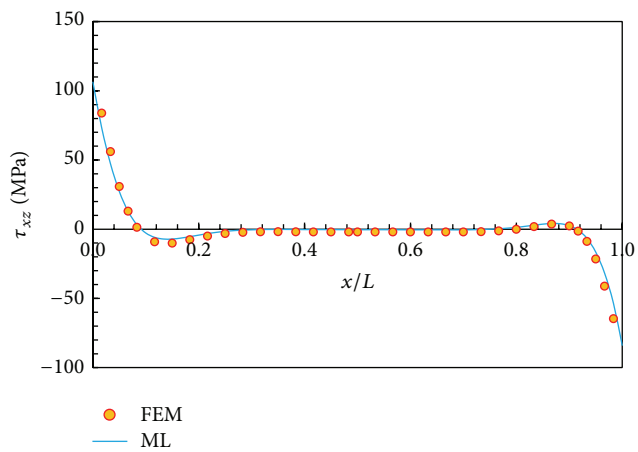

Figure 8: Shear stress distribution in middle layer.

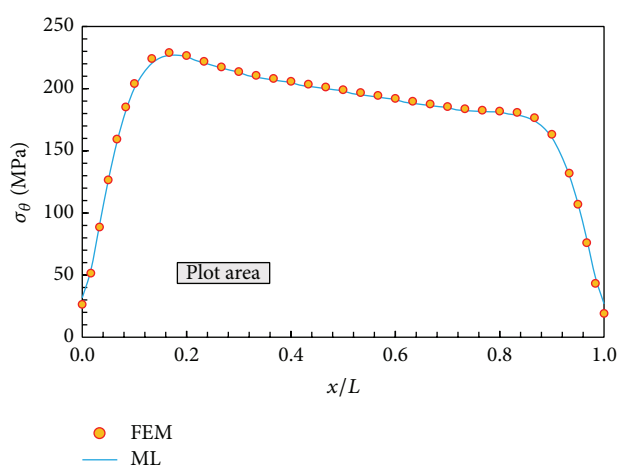

Figure 7: Circumferential stress distribution in middle layer.

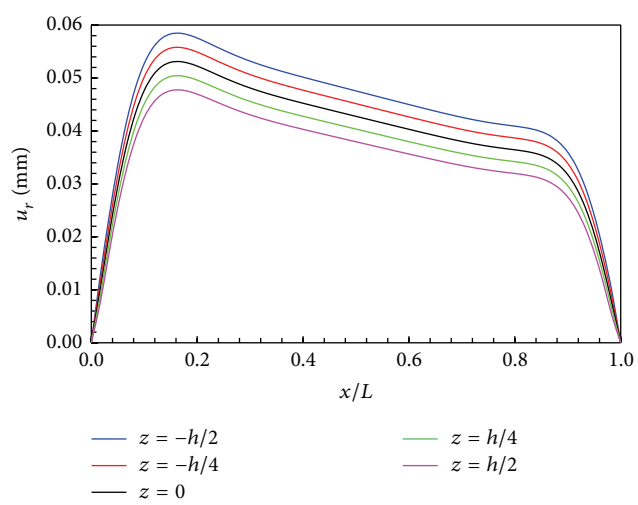

Figure 9: Radial displacement distribution in different layers.

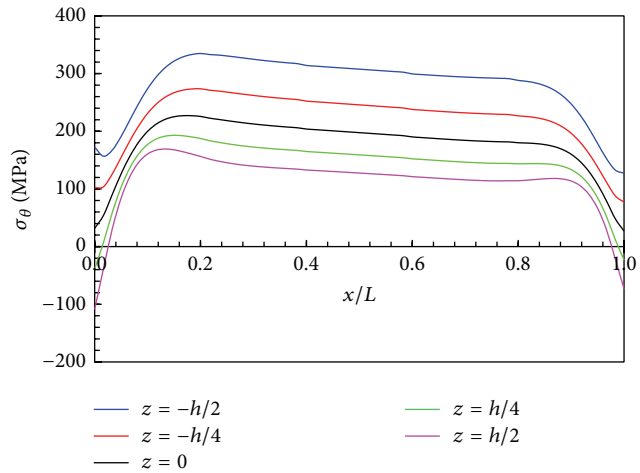

FIGURE 10: Circumferential stress distribution in different layers.

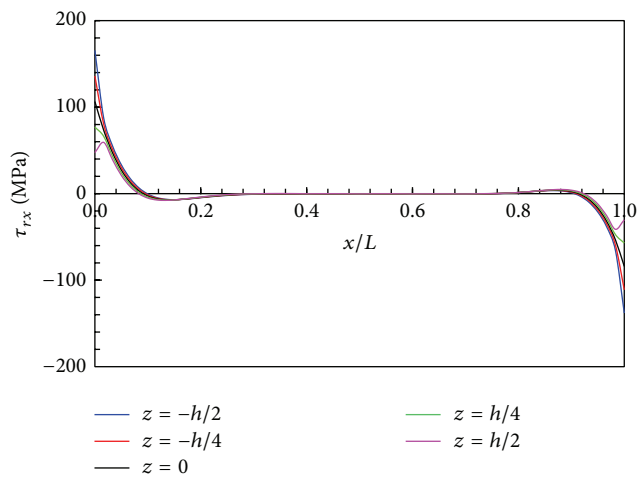

FIGURE 11: Shear stress distribution in different layers.

where U is the total strain energy of the elastic body and W is the total work of external forces due to internal pressure and centrifugal force.

With substituting strain energy and work of external forces, we have [10]

$$\begin{aligned}
&\int_0^L R \int_{-h/2}^{h/2} \left(\sigma_x \delta\varepsilon_x + \sigma_\theta \delta\varepsilon_\theta + \sigma_z \delta\varepsilon_z + \tau_{xz}\delta\gamma_{xz}\right) \\
&\qquad \times \left(1 + \frac{z}{R}\right) dz\, dx \\
&= \int_0^L \left(P_x \delta U_x + P_z \delta U_z\right)\left(R - \frac{h}{2}\right) dx \\
&\quad - \rho\omega^2 \int_0^L \int_{-h/2}^{h/2} (R+z)^2 \delta U_z dz\, dx.
\end{aligned} \tag{11}$$

Here ρ stands for the mass density, ω is the constant angular velocity, and $\rho\omega^2$ is the force per unit volume due to centrifugal force. Substituting (6) and (7) into (11) and

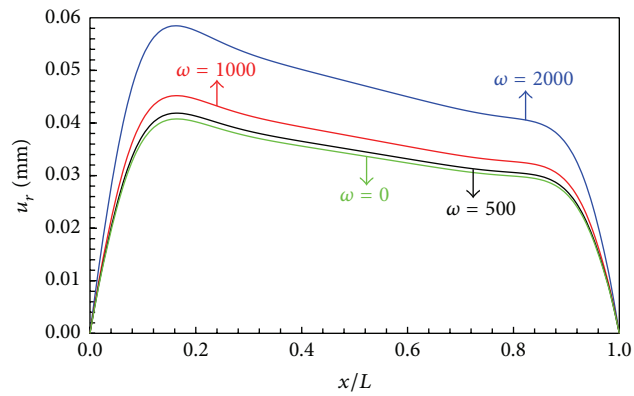

FIGURE 12: Radial displacement distribution in inner layer.

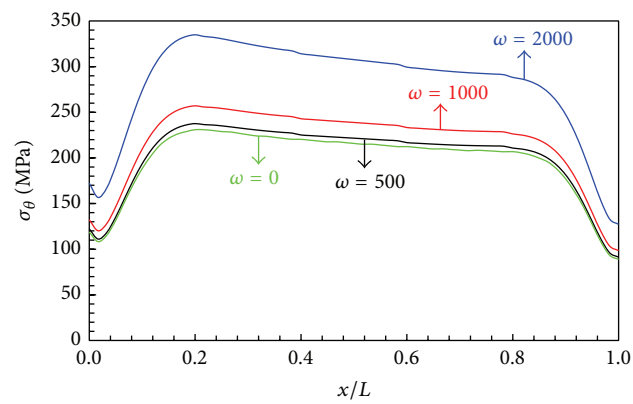

FIGURE 13: Circumferential stress distribution in inner layer.

drawing upon calculus of variation and the virtual work principle, we will have

$$\begin{aligned}
N_x R &= -\int P_x \left(R - \frac{h}{2}\right) dx + C_0, \\
M_x \frac{dR}{dx} + R\left(\frac{dM_x}{dx} - Q_x\right) &= P_x \frac{h}{2}\left(R - \frac{h}{2}\right), \\
Q_x \frac{dR}{dx} + R\left(\frac{dQ_x}{dx}\right) - N_\theta & \\
= -P_z\left(R - \frac{h}{2}\right) - \frac{\rho\omega^2}{6}\frac{h}{2}\left(12R^2 + h^2\right), & \\
M_{xz}\frac{dR}{dx} + R\left(\frac{dM_{xz}}{dx} - N_z\right) - M_\theta & \\
= P_z \frac{h}{2}\left(R - \frac{h}{2}\right) - \frac{\rho\omega^2}{6} R h^3, &
\end{aligned} \tag{12}$$

and the boundary conditions are

$$\left[\left(N_x \delta u + M_x \delta\phi + Q_x \delta w + M_{xz}\delta\psi\right) R\right]_0^L = 0. \tag{13}$$

Equation (13) states the boundary conditions which must exist at the two ends of the cone.

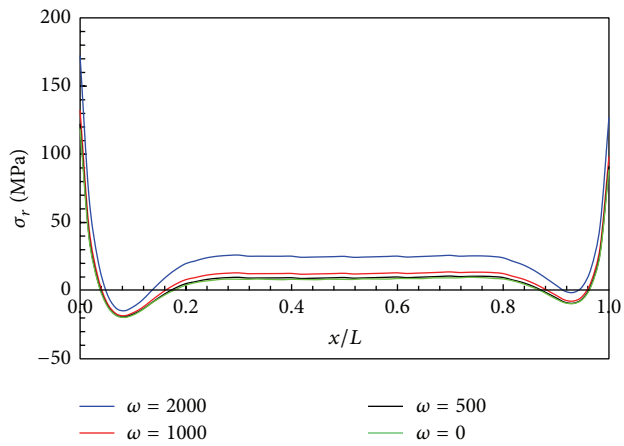

Figure 14: Radial stress distribution in inner layer.

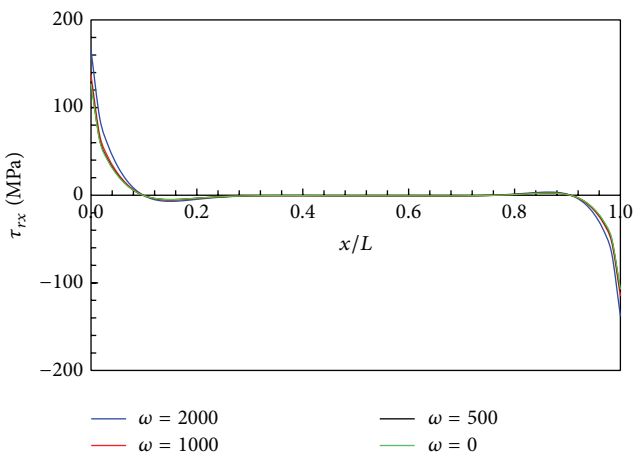

Figure 15: Shear stress distribution in inner layer.

In order to solve the set of differential equations (12), with using (6) to (9) and then using (12), we have

$$[B_1]\frac{d^2}{dx^2}\{y\}+[B_2]\frac{d}{dx}\{y\}+[B_3]\{y\}=\{F\},$$
$$\{y\}=\left\{\frac{du}{dx}\ \ \phi\ \ w\ \ \psi\right\}^T. \tag{14}$$

The coefficients matrices $[B_i]_{4\times4}$ and force vector $\{F\}_{4\times1}$ are as follows:

$$[B_1]=\begin{bmatrix}0 & 0 & 0 & 0\\ 0 & (1-v)\dfrac{h^3}{12}R & 0 & 0\\ 0 & 0 & \mu hR & \dfrac{\mu h^3}{12}\\ 0 & 0 & \dfrac{\mu h^3}{12} & \dfrac{\mu h^3}{12}R\end{bmatrix},$$

$$[B_2]=\begin{bmatrix}0 & (1-v)\dfrac{h^3}{12} & 0 & 0\\ (1-v)\dfrac{h^3}{12} & (1-v)\dfrac{h^3}{12}\dfrac{dR}{dx} & -\mu hR & -(\mu-2v)\dfrac{h^3}{12}\\ 0 & \mu hR & \mu h\dfrac{dR}{dx} & 0\\ 0 & (\mu-2v)\dfrac{h^3}{12} & 0 & \dfrac{\mu h^3}{12}\dfrac{dR}{dx}\end{bmatrix},$$

$$[B_3]=\begin{bmatrix}(1-v)hR & 0 & vh & vhR\\ 0 & -\mu hR & 0 & 0\\ -vh & \mu h\dfrac{dR}{dx} & -(1-v)\alpha & -h+(1-v)\alpha R\\ -vhR & 0 & -h+(1-v)\alpha R & -(1-v)\alpha R^2\end{bmatrix},$$

$$\{F\}=\frac{1}{\lambda}\begin{Bmatrix}-\int P_x\left(R-\dfrac{h}{2}\right)dx+C_0\\ P_x\dfrac{h}{2}\left(R-\dfrac{h}{2}\right)\\ -P_z\left(R-\dfrac{h}{2}\right)-\dfrac{\rho\omega^2}{6}\dfrac{h}{2}\left(12R^2+h^2\right)\\ P_z\dfrac{h}{2}\left(R-\dfrac{h}{2}\right)-\dfrac{\rho\omega^2}{6}Rh^3\end{Bmatrix}, \tag{15}$$

where the parameters are as follows:

$$\mu=\frac{5}{12}(1-2v),$$
$$\alpha=\ln\left(\frac{R+h/2}{R-h/2}\right). \tag{16}$$

The set of differential equations (14) is solved by perturbation technique in [10]. In the next section, a new method is presented for solving set of equation (12).

3. Solution with Disk Form Multilayers

In this method, the truncated cone is divided to disk layers with constant thickness t and constant height h (Figure 2).

Therefore, the governing equations convert to nonhomogeneous set of differential equations with constant coefficients. $x^{[k]}$ and $R^{[k]}$ are length and radius of middle of disks. k is number of disks. The modulus of elasticity and Poisson's ratio of disks are assumed be constant.

The length of middle of an arbitrary disk (Figure 3) is as follows:

$$x^{[k]} = \left(k - \frac{1}{2}\right)\frac{L}{n},$$
$$\left(x^{[k]} - \frac{t}{2}\right) \le x \le \left(x^{[k]} + \frac{t}{2}\right), \tag{17}$$
$$t = \frac{L}{n},$$

where n is the number of disks and k is the corresponding number given to each disk.

The radius of middle point of each disk is as follows:

$$R^{[k]} = a + \frac{h}{2} - (\tan\beta)\, x^{[k]}. \tag{18}$$

Thus

$$\left(\frac{dR}{dx}\right)^{[k]} = \frac{dR^{[k]}}{dx^{[k]}} = -\tan\beta. \tag{19}$$

With considering shear stress and based on FSDT, nonhomogeneous set of ordinary differential equations with constant coefficient of each disk is obtained. Consider

$$[B_1]^{[k]}\frac{d^2}{dx^2}\{y\}^{[k]} + [B_2]^{[k]}\frac{d}{dx}\{y\}^{[k]} + [B_3]^{[k]}\{y\}^{[k]} = \{F\}^{[k]},$$
$$\{y\}^{[k]} = \begin{Bmatrix} \left(\dfrac{du}{dx}\right)^{[k]} \\ \phi^{[k]} \\ w^{[k]} \\ \psi^{[k]} \end{Bmatrix}. \tag{20}$$

The coefficients matrices $[B_i]^{[k]}_{4\times4}$ and force vector $\{F\}^{k}_{4\times1}$ are as follows:

$$[B_1]^{[k]} = \begin{bmatrix} 0 & 0 & 0 & 0 \\ 0 & (1-\upsilon)\dfrac{h^3}{12}R^{[k]} & 0 & 0 \\ 0 & 0 & \mu h R^{[k]} & \dfrac{\mu h^3}{12} \\ 0 & 0 & \dfrac{\mu h^3}{12} & \dfrac{\mu h^3}{12}R^{[k]} \end{bmatrix},$$
$$[B_2]^{[k]} = \begin{bmatrix} 0 & (1-\upsilon)\dfrac{h^3}{12} & 0 & 0 \\ (1-\upsilon)\dfrac{h^3}{12} & -(1-\upsilon)\dfrac{h^3}{12}\tan\beta & -\mu h R^{[k]} & -(\mu-2\upsilon)\dfrac{h^3}{12} \\ 0 & \mu h R^{[k]} & -\mu h\tan\beta & 0 \\ 0 & (\mu-2\upsilon)\dfrac{h^3}{12} & 0 & -\dfrac{\mu h^3}{12}\tan\beta \end{bmatrix},$$
$$[B_3]^{[k]} = \begin{bmatrix} (1-\upsilon)hR^{[k]} & 0 & \upsilon h & \upsilon h R^{[k]} \\ 0 & -\mu h R^{[k]} & 0 & 0 \\ -\upsilon h & -\mu h\tan\beta & -(1-\upsilon)\alpha^{[k]} & -h + (1-\upsilon)\alpha^{[k]}R^{[k]} \\ -\upsilon h R^{[k]} & 0 & -h + (1-\upsilon)\alpha^{[k]}R^{[k]} & -(1-\upsilon)\alpha^{[k]}\left(R^{[k]}\right)^2 \end{bmatrix}, \tag{21}$$
$$\{F\}^{[k]} = \frac{1}{\lambda}\begin{Bmatrix} -P\sin\beta\left(R^{[k]} - \dfrac{h}{2}\right)x + C_0 \\ \dfrac{Ph}{2}\left(R^{[k]} - \dfrac{h}{2}\right)\sin\beta \\ -P\left(R^{[k]} - \dfrac{h}{2}\right)\cos\beta - \dfrac{\rho\omega^2}{6}\dfrac{h}{2}\left(12\left(R^{[k]}\right)^2 + h^2\right) \\ \dfrac{Ph}{2}\left(R^{[k]} - \dfrac{h}{2}\right)\cos\beta - \dfrac{\rho\omega^2}{6}h^3R^{[k]} \end{Bmatrix},$$

where the parameters are as follows

$$\mu = \frac{5}{12}(1-2\upsilon), \qquad \alpha^{[k]} = \ln\left(\frac{R^{[k]}+h/2}{R^{[k]}-h/2}\right). \tag{22}$$

Defining the differential operator $P(D)$, (20) is written as

$$[P(D)]^{[k]} = [B_1]^{[k]}D^2 + [B_2]^{[k]}D + [B_3]^{[k]}, \qquad D^2 = \frac{d^2}{dx^2}, \quad D = \frac{d}{dx}. \tag{23}$$

Thus

$$[P(D)]^{[k]}\{y\}^{[k]} = \{F\}^{[k]}. \tag{24}$$

The above differential equation has the total solution including general solution for homogeneous case $\{y\}_h^{[k]}$ and particular solution $\{y\}_p^{[k]}$ as follows:

$$\{y\}^{[k]} = \{y\}_h^{[k]} + \{y\}_p^{[k]}. \tag{25}$$

For the general solution for homogeneous case, $\{y\}_h^{[k]} = \{V\}^{[k]}e^{m^{[k]}x}$ is substituted in $[P(D)]^{[k]}\{y\}^{[k]} = 0$. Consider

$$\left|m^2[B_1]^{[k]} + m[B_2]^{[k]} + [B_3]^{[k]}\right| = 0. \tag{26}$$

Thus

$$\begin{vmatrix} B_{11} & B_{12} & B_{13} & B_{14} \\ B_{21} & B_{22} & B_{23} & B_{24} \\ B_{31} & B_{32} & B_{33} & B_{34} \\ B_{41} & B_{42} & B_{43} & B_{44} \end{vmatrix} = 0,$$

$$B_{11} = (1-\upsilon)hR^{[k]},$$

$$B_{12} = B_{21} = m(1-\upsilon)\frac{h^3}{12},$$

$$B_{13} = -B_{31} = \upsilon h,$$

$$B_{14} = -B_{41} = \upsilon hR^{[k]},$$

$$B_{22} = m^2(1-\upsilon)\frac{h^3}{12}R^{[k]} - m(1-\upsilon)\frac{h^3}{12}\tan\beta - \mu hR^{[k]},$$

$$B_{23} = -m\mu hR^{[k]},$$

$$B_{24} = -B_{42} = -m(\mu-2\upsilon)\frac{h^3}{12},$$

$$B_{32} = m\mu hR^{[k]} - \mu h\tan\beta,$$

$$B_{33} = m^2\mu hR^{[k]} - m\mu h\tan\beta - (1-\upsilon)\alpha^{[k]},$$

$$B_{34} = B_{43} = m^2\frac{\mu h^3}{12} - h + (1-\upsilon)\alpha^{[k]}R^{[k]},$$

$$B_{44} = m^2\frac{\mu h^3}{12}R^{[k]} - m\frac{\mu h^3}{12}\tan\beta - (1-\upsilon)\alpha^{[k]}\left(R^{[k]}\right)^2. \tag{27}$$

The result of the determinant above is a six-order polynomial which is a function of m, the solution of which is 6 eigenvalues m_i. The eigenvalues are 3 pairs of conjugated root. Substituting the calculated eigenvalues in the following equation, the corresponding eigenvectors $\{V\}_i$ are obtained. Consider

$$\left[m^2[B_1]^{[k]} + m[B_2]^{[k]} + [B_3]^{[k]}\right]\{V\}^{[k]} = 0. \tag{28}$$

Therefore, the homogeneous solutionis

$$\{y\}_h^{[k]} = \sum_{i=1}^{6} C_i^{[k]}\{V\}_i^{[k]}e^{m_i^{[k]}x}. \tag{29}$$

The particular solution is obtained as follows:

$$\{y\}_p^{[k]} = \left[[B_3]^{[k]}\right]^{-1}\{F\}^{[k]}. \tag{30}$$

Therefore, the total solutionis

$$\{y\}^{[k]} = \sum_{i=1}^{6} C_i^{[k]}\{V\}_i^{[k]}e^{m_i^{[k]}x} + \left[[B_3]^{[k]}\right]^{-1}\{F\}^{[k]}. \tag{31}$$

In general, the problem for each disk consists of 8 unknown values of C_i, including C_0 (first equation (12)), C_1 to C_6 (31), and C_7 (equation $u^{[k]} = \int (du/dx)^{[k]}dx + C_7$).

4. Boundary and Continuity Conditions

4.1. Boundary Conditions. In this problem, the boundary conditions of cone are clamped-clamped ends; then we have

$$\begin{Bmatrix} u \\ \phi \\ w \\ \psi \end{Bmatrix}_{x=0} = \begin{Bmatrix} u \\ \phi \\ w \\ \psi \end{Bmatrix}_{x=L} = \begin{Bmatrix} 0 \\ 0 \\ 0 \\ 0 \end{Bmatrix}. \tag{32}$$

Therefore

$$\begin{Bmatrix} U_x(x,z) \\ U_z(x,z) \end{Bmatrix}_{x=0,L} = \begin{Bmatrix} 0 \\ 0 \end{Bmatrix}. \tag{33}$$

4.2. Continuity Conditions. Because of continuity and homogeneity of the cone, at the boundary between two layers, forces, stresses, and displacements must be continuous. Given that shear deformation theory applied is an approximation of one order and also all equations related to the stresses include

the first derivatives of displacement, the continuity conditions are as follows:

$$\begin{Bmatrix} U_x^{[k-1]}(x,z) \\ U_z^{[k-1]}(x,z) \end{Bmatrix}_{x=x^{[k-1]}+t/2} = \begin{Bmatrix} U_x^{[k]}(x,z) \\ U_z^{[k]}(x,z) \end{Bmatrix}_{x=x^{[k]}-t/2},$$

$$\begin{Bmatrix} U_x^{[k]}(x,z) \\ U_z^{[k]}(x,z) \end{Bmatrix}_{x=x^{[k]}+t/2} = \begin{Bmatrix} U_x^{[k+1]}(x,z) \\ U_z^{[k+1]}(x,z) \end{Bmatrix}_{x=x^{[k+1]}-t/2},$$

$$\begin{Bmatrix} \dfrac{dU_x^{[k-1]}(x,z)}{dx} \\ \dfrac{dU_z^{[k-1]}(x,z)}{dx} \end{Bmatrix}_{x=x^{[k-1]}+t/2} = \begin{Bmatrix} \dfrac{dU_x^{[k]}(x,z)}{dx} \\ \dfrac{dU_z^{[k]}(x,z)}{dx} \end{Bmatrix}_{x=x^{[k]}-t/2},$$

$$\begin{Bmatrix} \dfrac{dU_x^{[k]}(x,z)}{dx} \\ \dfrac{dU_z^{[k]}(x,z)}{dx} \end{Bmatrix}_{x=x^{[k]}+t/2} = \begin{Bmatrix} \dfrac{dU_x^{[k+1]}(x,z)}{dx} \\ \dfrac{dU_z^{[k+1]}(x,z)}{dx} \end{Bmatrix}_{x=x^{[k+1]}-t/2}. \tag{34}$$

Given the continuity conditions, in terms of z, 8 equations are obtained. In general, if the cone is divided into n disk layers, $8(n-1)$ equations are obtained. Using the 8 equations of boundary condition, $8n$ equations are obtained. The solution of these equations yields $8n$ unknown constants.

5. Results and Discussion

The solution described in the preceding section for a homogeneous and isotropic truncated conical shell with $a = 40$ mm, $b = 30$ mm, $h = 20$ mm, and $L = 400$ mm will be considered. Young's Modulus and Poisson's ratio, respectively, have values of $E = 200$ GPa and $\upsilon = 0.3$. The applied internal pressure is 80 MPa. The truncated cone rotates with $\omega = 2000$ rad/s and has clamped-clamped boundary conditions.

The effect of the number of disk layers on the radial displacement is shown in Figure 4. It is observed that, if the number of disk layers is fewer than 30, it will have a significant effect on the response. However, if the number of layers is more than 40 disks, there will be no significant effect on radial displacement. In the problem in question 60 disks are used.

In Figures 5, 6, 7, and 8, displacement and stress distributions are obtained using multilayer method (ML), are compared with the solutions of FEM, and are presented in the form of graphs. Figures 9, 10, 11, and 12 show that the disk layer method based on FSDT has an acceptable amount of accuracy when one wants to obtain radial displacement, radial stress, circumferential stress, and shear stress.

The distribution of radial displacement at different layers is plotted in Figure 9. The radial displacement at points away from the boundaries depends on radius and length. According to Figure 9, the change in radial displacement in the lower boundary is greater than that of the upper boundary and the greatest radial displacement occurs in the internal surface ($z = -h/2$).

Distribution of circumferential stress in different layers is shown in Figure 10. The circumferential stress at all points depends on radius and length. The circumferential stress at layers close to the external surface is negative and at other layers positive. The greatest circumferential stress occurs in the internal surface ($z = -h/2$).

Figure 8 shows the distribution of shear stress at different layers. The shear stress at points away from the boundaries at different layers is the same and trivial. However, at points near the boundaries, the stress is significant, especially in the internal surface, which is the greatest.

The effects of angular velocity ω on the distribution of the stresses and radial displacement are presented in Figures 12, 13, 14, and 15. Results of Figures 12 to 15 can be summarized to conclude that displacement and stresses rise with increasing angular velocity. But the rate of changes at all points depends on radius and length.

From these four figures it is illustrated that for the angular speed less than 500 rad/s the centrifugal force is less effective than the internal pressure on the truncated cone.

6. Conclusions

Homogenous and isotropic thick-walled conical shells could be solved using the analytical method. First shear deformation theory and perturbation theory result in the analytical solution of the problem with higher accuracy and within a shorter period of time. However, the above-mentioned solutions are complicated and time-consuming. The multilayer disc form method could be a good replacement for the analysis of thick-walled shells. In this method, shells with different geometries and different loadings and different boundary conditions, with even variable pressure, could be more easily solved. This in spite of the fact that the existing analytical methods, due to their complex mathematical relations governing them could not easily solve them. The method presented is very suitable for the purpose of calculation of radial stress, circumferential stress, shear stress, and radial displacement.

Conflict of Interests

The authors declare that there is no conflict of interests regarding the publication of this paper.

References

[1] I. Mirsky and G. Hermann, "Axially motions of thick cylindrical shells," *Journal of Applied Mechanics*, vol. 25, pp. 97–102, 1958.

[2] G. F. Hausenbauer and G. C. Lee, "Stresses in thick-walled conical shells," *Nuclear Engineering and Design*, vol. 3, no. 3, pp. 394–401, 1966.

[3] I. S. Raju, G. V. Rao, B. P. Rao, and J. Venkataramana, "A conical shell finite element," *Computers and Structures*, vol. 4, no. 4, pp. 901–915, 1974.

[4] S. Takahashi, K. Suzuki, and T. Kosawada, "Vibrations of conical shells with variable thickness," *Bulletin of the JSME-Japan Society of Mechanical Engineers*, vol. 29, no. 258, pp. 4306–4311, 1986.

[5] B. S. K. Sundarasivarao and N. Ganesan, "Deformation of varying thickness of conical shells subjected to axisymmetric loading with various end conditions," *Engineering Fracture Mechanics*, vol. 39, no. 6, pp. 1003–1010, 1991.

[6] S. A. Tavares, "Thin conical shells with constant thickness and under axisymmetric load," *Computers and Structures*, vol. 60, no. 6, pp. 895–921, 1996.

[7] W. Cui, J. Pei, and W. Zhang, "Simple and accurate solution for calculating stresses in conical shells," *Computers and Structures*, vol. 79, no. 3, pp. 265–279, 2001.

[8] C.-P. Wu and S.-J. Chiu, "Thermally induced dynamic instability of laminated composite conical shells," *International Journal of Solids and Structures*, vol. 39, no. 11, pp. 3001–3021, 2002.

[9] I. F. Pinto Correia, C. M. Mota Soares, C. A. Mota Soares, and J. Herskovits, "Analysis of laminated conical shell structures using higher order models," *Composite Structures*, vol. 62, no. 3-4, pp. 383–390, 2003.

[10] K. C. Jane and Y. H. Wu, "A generalized thermoelasticity problem of multilayered conical shells," *International Journal of Solids and Structures*, vol. 41, no. 9-10, pp. 2205–2233, 2004.

[11] C.-P. Wu, Y.-F. Pu, and Y.-H. Tsai, "Asymptotic solutions of axisymmetric laminated conical shells," *Thin-Walled Structures*, vol. 43, no. 10, pp. 1589–1614, 2005.

[12] H. R. S. Eipakchi, E. Khadem, and G. H. S. Rahimi, "Axisymmetric stress analysis of a thick conical shell with varying thickness under nonuniform internal pressure," *Journal of Engineering Mechanics*, vol. 134, no. 8, pp. 601–610, 2008.

[13] M. Ghannad, M. Z. Nejad, and G. H. Rahimi, "Elastic solution of axisymmetric thick truncated conical shells based on first-order shear deformation theory," *Mechanika*, vol. 79, no. 5, pp. 13–20, 2009.

[14] M. Z. Nejad, G. H. Rahimi, and M. Ghannad, "Set of field equations for thick shell of revolution made of functionally graded materials in curvilinear coordinate system," *Mechanika*, vol. 77, no. 3, pp. 18–26, 2009.

[15] A. V. Borisov, "Elastic analysis of multilayered thick-walled spheres under external load," *Mechanika*, vol. 84, no. 4, pp. 28–32, 2010.

[16] H. R. Eipakchi, "Third-order shear deformation theory for stress analysis of a thick conical shell under pressure," *Journal of Mechanics of Materials and Structures*, vol. 5, no. 1, pp. 1–17, 2010.

[17] K. Asemi, M. Akhlaghi, M. Salehi, and S. K. Hosseini Zad, "Analysis of functionally graded thick truncated cone with finite length under hydrostatic internal pressure," *Archive of Applied Mechanics*, vol. 81, no. 8, pp. 1063–1074, 2011.

[18] M. Ghannad and M. Zamani Nejad, "Elastic analysis of pressurized thick hollow cylindrical shells with clamped-clamped ends," *Mechanika*, vol. 85, no. 5, pp. 11–18, 2010.

[19] F. Shadmehri, S. V. Hoa, and M. Hojjati, "Buckling of conical composite shells," *Composite Structures*, vol. 94, no. 2, pp. 787–792, 2012.

[20] O. Civalek, "Vibration analysis of laminated composite conical shells by the method of discrete singular convolution based on the shear deformation theory," *Composites Part B-Engineering*, vol. 45, pp. 1001–1009, 2013.

[21] M. Z. Nejad, M. Jabbari, and M. Ghannad, "A semi-analytical solution for elastic analysis of rotating thick cylindrical shells with variable thickness using disk form multilayers," *The Scientific World Journal*, vol. 2014, Article ID 932743, 10 pages, 2014.

[22] S. Vlachoutsis, "Shear correction factors for plates and shells," *International Journal for Numerical Methods in Engineering*, vol. 33, no. 7, pp. 1537–1552, 1992.